Obstacle-Aided Locomotion of a Snake Robot Using Piecewise Helixes

doi: 10.1109/LRA.2022.3194689

Obstacle-Aided Locomotion of a Snake Robot Using Piecewise Helixes

Takuro Takanashi[1] , Mizuki Nakajima[1], Tatsuya Takemori[2], and Motoyasu Tanaka[1]

***Abstract*—A non-wheeled snake robot can propel itself by pushing against obstacles. This is called obstacle-aided locomotion. To expand the exploration range of a snake robot using this method, it is preferable to utilize obstacles that are both on the ground and by the side or above. To achieve these goals, we propose an obstacle-aided locomotion using piecewise helixes. This target shape comprises grounding and obstacle-contacting parts. The length and shape of the grounding part can be changed from a straight line to a circular arc. The height of the obstacle-contacting part can be changed or its direction can be reversed. The robot can adapt to various obstacles by appropriately changing its body shape. In addition, we propose a snake robot locomotion in a flat ground using the same shape as that used for obstacle-aided locomotion. This involves a combination of shift control and rolling motion. The robot can move in a straight line in the forward or lateral direction or can turn in a circular arc using the proposed method. Finally, experiments that confirm the effectiveness of the proposed method are presented.**

***Index Terms*—Field Robots, Search and Rescue Robots, Biologically-Inspired Robots.**

I. INTRODUCTION

SNAKE robots are expected to play an active role in the exploration of confined spaces, uneven environments, and complex environments that are inaccessible to humans. Various control methods have been studied to adapt to these environments [1-6]. In [1], various movements were realized, such as serpentine, sinus-lifting, and pedal wave. In [2], sidewinding performed by desert snakes was realized. Additionally, the modeling of the direction and velocity of this movement was proposed [3]. In addition, a method of moving by wrapping around pipes [4], climbing ladders [5], and ascending and descending steps [6] has been proposed using a slender body.

Numerous studies have focused on how to move efficiently using obstacles in complex environments [7-14]. In [7, 8], a method of propulsion by lateral undulation motion was proposed by controlling the link angle such that the reaction force and friction force generated at the three contact points between the snake robot and the obstacle were directed along the direction of travel. In [9], when a robot detects that it is stuck on an obstacle, it rotates the link receiving the contact force to increase the propulsive direction of the contact force of each link, thereby creating a contact state that is advantageous for obstacle-aided locomotion. A control method for maintaining contact with obstacles, which is important for obstacle-aided locomotion, has also been proposed [10,11]. In [12], the serpenoid function was extended to realize obstacle-aided locomotion by applying local shape-based compliance control in accordance with the contact with obstacles during motion. This method was extended further to identify obstacles that interfere with the robot's motion and improve the travel distance and speed by reacting more sensitively [13]. A method to continuously adjust the direction of movement and traverse obstacles using contact with them during sidewinding was proposed [14]. In [15], autonomous decentralized control was proposed, in which curvature derivative control [16] and a simple reflection mechanism were combined. It is confirmed that a robot could move using the obstacles by the method above in [17]. In addition, "Tegotae-based decentralized control," which utilizes only the reaction forces from obstacles that contribute to propulsion, has been proposed [18].

Most previous studies only considered obstacle environments on two-dimensional planes. However, at disaster sites where snake robots are expected to play an active role, three-dimensional environments, such as rubble and uneven ground, were considered. To adapt to these environments, several approaches were proposed. For example, propulsion generated by pushing against uneven ground [12, 13], obstacle avoidance by lifting a part of the robot [19], and mobility improvement by adding compliance elements between the robot's modules for better contact with the uneven ground [20] were introduced.

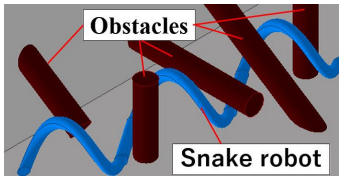

Fig. 1. Snake robot in a cluttered environment.

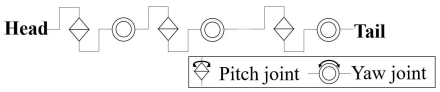

Fig. 2. Structure of a snake robot.

Manuscript received: February, 20, 2022; Revised June, 16, 2022; Accepted July, 10, 2022.

This paper was recommended for publication by Pauline Pounds upon evaluation of the Associate Editor and Reviewers' comments. This work was partially supported by JSPS KAKENHI Grant Numbers JP21H01285.

[1]T. Takanashi, M. Nakajima, and M. Tanaka are with the Department of Mechanical and Intelligent Systems Engineering, University of Electro-Communications, Tokyo 182-8585, Japan. takuro.takanashi@rc.mce.uec.ac.jp; mizuki.nakajima@rc.mce.uec.ac.jp; mtanaka@uec.ac.jp

[2]T. Takemori is with the Department of Mechanical Engineering and Science, Graduate School of Engineering, Kyoto University, Kyoto 606-8501, Japan. takemori.tatsuya.23a@st.kyoto-u.ac.jp

Digital Object Identifier (DOI): see top of this page.

Biological snakes adapt to three-dimensional terrains in several ways. In [21], it was reported that snakes use a combination of vertical and lateral bending to advance on uneven terrain for propulsion. The snake can lift parts of its body to overcome small undulations, and switching between multiple movements in response to vertical pegs. Additionally, sometimes it can come in contact with the pegs to propel itself or change direction [22]. Thus, it is suggested that snakes can adapt to three-dimensional environments by utilizing its slender body. This can be achieved by avoiding or using the obstacles, and/or adapting their own body shape to the terrain.

Previous studies have focused on ground environment on the underside of the biological snakes and snake robots. However, in environments with collapsed houses and industrial plants, obstacles, such as pipes and branches that lean against walls or protrude from the sides, exist. If there are few obstacles that can be used for propulsion, the range and path that can be promoted by obstacle-aided locomotion will be limited. Consequently, if obstacles at high places can be used for propulsion, the obstacle options available for obstacle-aided locomotion will increase and the search range will expand. Existing methods using two-dimensional body shape conrol such as lateral or vertical undulation do not work well when a snake robot utilizes obstacles at high places. This is because the robot may lose its balance during locomotion and fall over due to insufficient contact with the ground. In addition, it is known that contact with a vertically projecting obstacle with two-dimensional lateral bending of snake robot causes rotation and skidding, unless there is ground with enough firictional force [23].

In this study, we focused on obstacles located both on the ground and at high places. We proposed an obstacle-aided locomotion method, which uses piecewise helixes to improve the mobility of a snake robot in such environments. To design this target shape, we used the method proposed by Takemori [24] and Yamada [25]. Our method uses a three-dimensional shape as target shape to maintain contact with the obstacle at high places without falling. In addition, by making contact with a vertically protruding obstacle using a three-dimensional robot shape, the decomposition of the frictional force between the robot and the obstacle surface in a three-dimensional direction prevented the rotation and skidding to continue obstacle-aided locomotion. Furthermore, we proposed a method that enables the robot to move and turn in different directions, even in a flat environment without obstacles. In an environment where the snake robot is exploring, the snake robot may not be able to move by utilizing only obstacle-aided locomotion because there are no or few obstacles available. Consequently, to expand the exploration range of a snake robot that has no wheels or other propulsion mechanisms, a method that works under such environment is needed. This method should be easily switched to obstacle-aided locomotion without any change in body shape or control method. Consequently, as the second main contribution of this study, we proposed a method for moving and turning in any direction in a flat environment without obstacles. This method was achieved by combining the shift control and the rolling motion [25] with the same body shape and control method used for obstacle-aided locomotion.

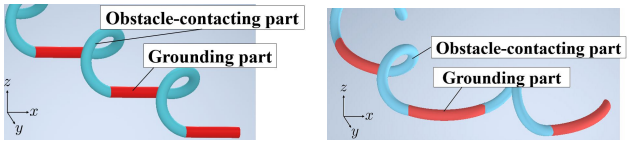

(a) Basic shape (b) Bending shape

Fig. 3. Segment configuration of piecewise helixes.

TABLE I
PARAMETERS OF SEGMENTS FOR THE TARGET SHAPE

seg no. j	part	shape	parameter
$2m+1$	Grounding part	Straight line Circular arc	(l_j, κ_j)
$2m+2$	Obstacle-contacting part	Elliptical Helix	(a_j, b_j, h_j, ϕ_j)

In this study, the interior of a collapsed house was assumed as the environment. The obstacles were assumed to be located both on the two-dimensional plane and at high places, such as pipes protruding from the side or above, as shown in Fig.1. The snake robot in this study had no wheels and comprised a pitch and yaw joints connected alternately, as shown in Fig.2. The length of the links were equal.

II. LOCOMOTION BY USING PIECEWISE HELIXES

The target shape of the robot is set to be a piecewise helixes that consists of obstacle-contacting parts and grounding parts that are alternately connected, as shown in Fig.3. Using this shape, the robot can perform not only obstacle-aided locomotion but also move and turn in various directions in a flat environment without obstacles. The obstacle-contacting part is used to push against the obstacle for locomotion. The grounding part is used to determine the direction of locomotion and the next obstacle to be aided. The grounding part can change its length and curvature, and the obstacle-contacting part can change its height and its direction of the connection with the grounding part. The robot uses these changes in body shape to adapt to the environment as it moves. To design the target shape, we used the method of approximating the body shape of a snake robot to a continuous curve proposed by Yamada [25] and the method of connecting simple shapes proposed by Takemori [24].

The parameters of each part are shown in Table I The target shape was formed by repeatedly connecting two segments. This unit of segments is called segment units, where $m \in \mathbb{Z}$ is the index of the segment unit. In Table I, the parameters listed are for the j-th segment. The obstacle-contacting part is an elliptical helix shape. The cross section of the elliptical helix on $x-z$ plane is shown in Fig.4a, where a_j is the length of the major axis of the ellipse and b_j the length of the minor axis. The elliptical helix is defined by tracing a vertical elliptic cylinder with a tilt angle h_j and its winding angle ϕ_j. The pitch of the helix p_j, i.e., the height of the helix in one revolution, was determined as $2\pi h_j$ (Fig.4b). The grounding part is defined by the length l_j and the curvature κ_j as shown in Fig.4c. By changing κ_j, the grounding part can form a straight line or a circular arc, as shown in Fig.3.

Sidewinding can be considered as rolling an elliptical helix [2, 3, 20, 22]. The basic shape of our method is similar to

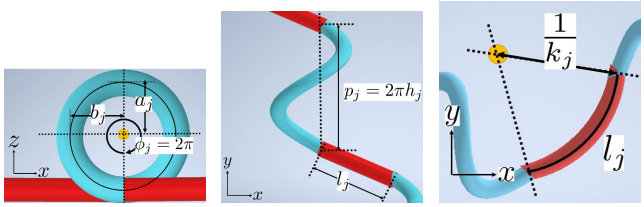

(a) Elliptical helix parameters (b) Definition of elliptical helix pitch (c) The curvature and length of the grounding part

Fig. 4. Parameters of target shape.

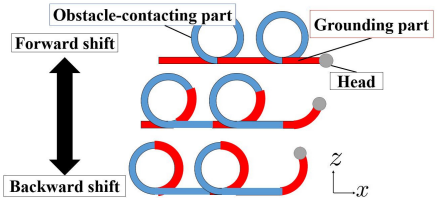

Fig. 5. Moving by shift control.

this movement because the shape of our method is composed of elliptical helixes and straight lines. However, our proposed method allows the parameters of each segment to be changed independently. Thus, it is possible to change the shape of each part, such as elongating the height of the elliptical helix, to allow contact with obstacles at high places while maintaining or changing the grounding part. This enables the robot to balance its posture during movement and adapt to different obstacle environments.

A. Obstacle-Aided Locomotion

Locomotion was performed using the shift control method. When shift control was applied, the entire robot moved, as shown in Fig. 5. The motion in which the robot moves toward the front is called a forward shift, and the motion in which the robot moves toward the rear is called a backward shift.

As shown in Fig.6, obstacle-aided locomotion is performed by contacting the obstacle on one side of the obstacle-contacting part. As shown in Fig.6, when the robot is in contact with an obstacle, it moves in the head direction using backward shift.

1) Adaptation to Obstacle Environments Using Body Shape Changes: To adapt to various obstacle environments, the robot performs body shape changes such as extending and bending the grounding part, reversing the obstacle-contacting part, and adjusting the height. The body shape of the robot is changed to ensure the obstacle-contacting part has a proper contact with the obstacle. In this method, the following conditions are required for obstacle-aided locomotion.

- The robot is always in contact with two or more obstacles to the obstacle-aided locomotion.
- When changing body shape of the robot, the operator must be able to see the first obstacle-contacting part.

Fig.7a-(c) shows the extending, bending, and shortening of the grounding part. These shape changes are used when

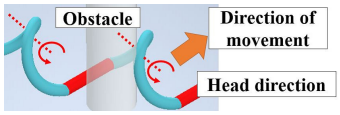

Fig. 6. Obstacle-aided locomotion.

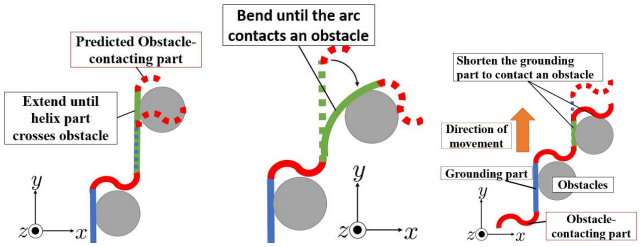

(a) Extending of the grounding part (b) Bending of the grounding part (c) Shortening of the grounding part

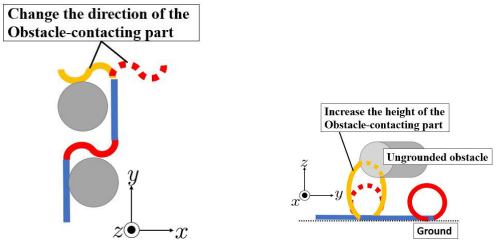

(d) Reversal of the obstacle-contacting part (e) Height adjustment of the obstacle-contacting part

Fig. 7. Body shape changes.

choosing the travel direction and obstacle to be utilized as well as when optimizing the contact with it. The shape of the grounding part is changed when the predicted obstacle-contacting part interferes with the obstacle (Fig.7a), when the grounding part is away from the obstacle (Fig.7b), and when the obstacle-contacting part is away from the obstacle (Fig.7c), respectively. These are used to adjust the position of the leading obstacle-contacting part so that the obstacle can be used for locomotion.

In Fig.7d, the reversal of the obstacle-contacting part is performed when the obstacle is on the opposite side. The height of the obstacle-contacting part is adjusted when the obstacle is located at a high place and a contact cannot be made (Fig.7e).

These body-shape changes were performed only in the first segment of the robot.

2) Conditions for Maintaining Contact with Obstacles: Contact with obstacles must be maintained for obstacle-aided locomotion. In our method, the ease of maintaining contact depends on the contact condition between the robot and obstacle. In this section, we describe the conditions for maintaining contact at each point of the obstacle-contacting part with the obstacle.

It is assumed that the shape of the obstacle is circular, as shown in Fig.8; the robot is in contact with the obstacle at two points: the grounding part and the obstacle-contacting part. We assume that the robot moves under the reaction force N

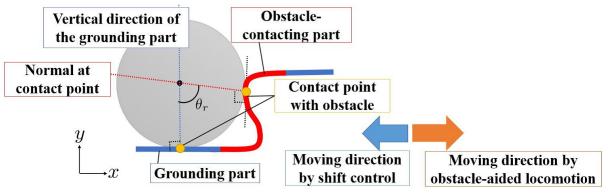

Fig. 8. Contacting points between the robot and the obstacle.

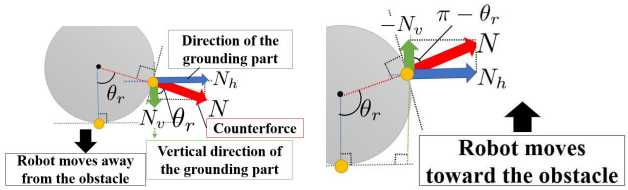

(a) (b)

Fig. 9. Comparison of two reaction force cases received from the contact of obstacle-contacting parts. (a) When $\theta_r < \pi/2$, the robot moves away from the obstacle. (b) When $\theta_r > \pi/2$, the robot moves in the direction of the obstacle to maintain contact for obstacle-aided locomotion.

received from the obstacle-contacting part's contact point, as shown in Fig.9; the reaction force received at the contact point with the grounding part is not considered. We also assume that the robot is in contact with more than one obstacle and does not rotate. Let θ_r be the angle between the normal at the point of contact with the obstacle and the line passing through the point of contact with the grounding part and perpendicular to the longitudinal direction of the grounding part, as shown in Fig.8 and Fig. 9. The components of the reaction force in the length direction of the grounding part N_h and in the direction perpendicular to it N_v are obtained as $N_h = N\sin\theta_r$ and $N_v = N\cos\theta_r$.

Fig.9 shows two conditions of θ_r, where $\theta_r < \pi/2$ and $\theta_r > \pi/2$. The direction of N_v moves the robot away from the obstacle when $\theta_r < \pi/2$ (Fig.9b), whereas it moves the robot toward the obstacle when $\theta_r > \pi/2$. The robot must move in the direction toward the obstacle to maintain contact for obstacle-aided locomotion; therefore, the condition $\theta_r > \pi/2$ should be fulfilled.

Even when the contact is with an obstacle that is not a perfect circle or flat surface, the angle θ_r can be calculated if the normal direction of the point of contact between the obstacle and the obstacle-contacting part is known; further, the contact maintenance condition can be determined.

As shown in Fig.10a, the direction of the friction force from the obstacle also differs because the robot moves in different directions on the obstacle surface depending on the contact point. The component of the friction force, z'_h, which is perpendicular to the longitudinal direction of the grounding part, is the force with which the robot moves away from the obstacle. In this section, we explain the condition of the contact point in the obstacle-contacting part to maintain contact with the obstacle.

Consider the case in which the obstacle-contacting part is viewed in z'_h–y_h plane perpendicular to the longitudinal direction of the grounding part, as shown in Fig. 10a. We

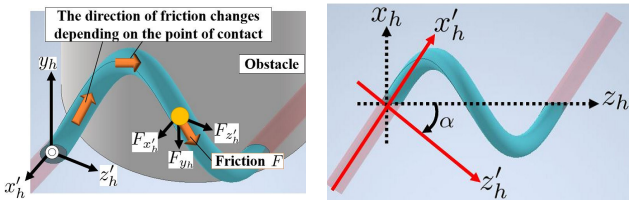

(a) Direction of friction force (b) Coordinate transformation

Fig. 10. Direction of friction force by contact point.

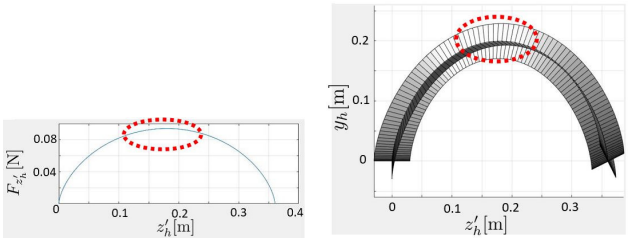

(a) Graph showing the variation of $F_{z'_h}$ with z'_h (b) Backbone curve of the obstacle-contacting part

Fig. 11. Undesirable contact points when $F = 0.1, h = 0.07, r_h = 0.1$.

assume that the obstacle-contacting part is an ordinary helix with a radius r_h and tilt angle h. The helix in the (x_h, y_h, z_h) coordinate system as shown in Fig.10b is obtained using a mediator ϕ_j as follows:

$$\begin{cases} x_h = r_h \sin\phi_j \\ y_h = r_h \cos\phi_j \\ z_h = h\phi_j \end{cases}. \tag{1}$$

The vector in the direction of the robot body axis in the (x_h, y_h, z_h) coordinate system is obtained by differentiating (1) with respect to ϕ_j as follows:

$$\begin{bmatrix} \Delta x_h \\ \Delta y_h \\ \Delta z_h \end{bmatrix} = \begin{bmatrix} r_h \cos\phi_j \\ -r_h \sin\phi_j \\ h \end{bmatrix}. \tag{2}$$

To transform (2) to the coordinate system in Fig.10a, we must rotate the coordinate system around the y-axis by $\alpha = \tan^{-1}(h/r_h)$, as shown in Fig.10b. The vector in the direction of the robot body axis in the (x'_h, y_h, z'_h) coordinate system after the coordinate transformation can be obtained as follows:

$$\begin{bmatrix} \Delta x'_h \\ \Delta y_h \\ \Delta z'_h \end{bmatrix} = \begin{bmatrix} h\sin\alpha + r_h\cos\phi_j\cos\alpha \\ -r_h\sin\phi_j \\ h\cos\alpha - r_h\cos\phi_j\sin\alpha \end{bmatrix}. \tag{3}$$

Assuming that a constant frictional force F acts in the direction of the robot body axes, the frictional force $(F_{x'_h}, F_{y_h}, F_{z'_h})$ in each direction can be obtained using the unit vector in (3) as follows:

$$\begin{bmatrix} F_{x'_h} \\ F_{y_h} \\ F_{z'_h} \end{bmatrix} = F \cdot \frac{1}{\sqrt{{\Delta x'_h}^2 + \Delta y_h^2 + {\Delta x'_h}^2}} \begin{bmatrix} \Delta x'_h \\ \Delta y_h \\ \Delta z'_h \end{bmatrix}. \tag{4}$$

The variation in the frictional force $F_{z'_h}$ in the direction of z'_h is shown in the graph in Fig.11a, where the radius of the

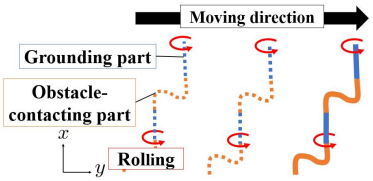

Fig. 12. Moving by rolling.

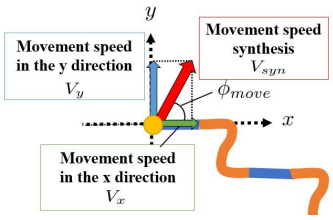

Fig. 13. Movement speed synthesis.

helix (r_h) is 0.1 m, the tilt angle of the helix (h) is 0.07 m, and the friction force (F) is tentatively set to 0.1 N. This graph shows that the value of $F_{z'_h}$ is particularly large near the center of the obstacle-contacting part (the area within the red dotted line in Fig. 11). When the robot contacts an obstacle in this area, it is likely to move away from the obstacle. Therefore, ideally, this area must be avoided to maintain contact with obstacles.

In the proposed method of obstacle-aided locomotion, the contact points on the obstacle and the obstacle-contacting part must be adjusted appropriately so that the conditions mentioned above can be satisfied.

B. Moving in a Flat Environment without Obstacles

If the shift control method (Fig.5) and rolling (Fig.12) are combined, the robot can move in any direction in a flat environment without obstacles. Shift control is performed by changing the region corresponding to the body of the robot in the target curve. By using this control method, the robot can smoothly change its body shape. Let s_h be the head position of the snake robot and $\dot{s}_h$ be the propagation velocity of the head on the target curve. Additionally, let the rolling be a rotational motion with angular velocity ω_{roll} when the robot's body is considered to be a cylinder. In this section, the relationship between the moving speed using shift control $\dot{s}_h$ and rolling ω_{roll} is determined such that the robot moves in any direction in a flat environment.

As shown in Fig.13, it is assumed that the grounding part is a straight line, and that the x-axis and y-axis are its longitudinal and perpendicular directions, respectively. The velocity components V_x and V_y in the x and y axis directions during simultaneous shift control and rolling motion can be obtained using the arbitrary velocity V_{syn} and angle ϕ_{move}, which is the angle between the x-axis and the direction of movement, as follows :

$$\begin{cases} V_x = V_{syn} \cdot \cos\phi_{move}, \\ V_y = V_{syn} \cdot \sin\phi_{move}. \end{cases} \tag{5}$$

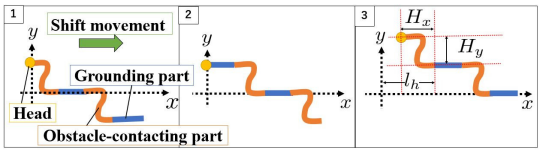

Fig. 14. Movement of the head of one cycle by shift control.

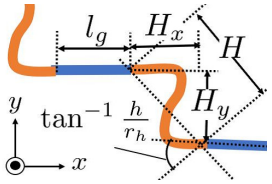

Fig. 15. Parameters of the helix decomposed in the x-y direction.

As shown in Fig.14, let l_h be the length of the obstacle-contacting part when it is straightened by untying, and H_x and H_y be the heights of the helix $H = 2\pi h$ decomposed over the direction of body axis of the grounding part x and perpendicular to it y axes, respectively (Fig.15). The displacement of the head in the x-axis is $(l_h - H_x)$, and the displacement in the y-axis is H_y in one cycle when only shift control is performed. When rolling motion is added, the average velocity in the x and y axis directions V_x and V_y are obtained by dividing the amount of movement in each direction for one cycle by the travel time, as follows:

$$\begin{cases} V_x = (l_h - H_x) \cdot \frac{\dot{s}_h}{l_h + l_g}, \\ V_y = H_y \cdot \frac{\dot{s}_h}{l_h + l_g} + \omega_{roll} \cdot R_{link}, \end{cases} \tag{6}$$

where l_g denote the length of the grounding part, and R_{link} is the radius of the robot's link.

For movement in any direction ϕ_{move} with a moving speed V_{syn}, $\dot{s}_h$ and ω_{roll} can be determined by deriving (5) and (6) as follows:

$$\dot{s}_h = \frac{l_h + l_g}{l_h - H_x} \cdot V_{syn} \cdot \cos\phi_{move} \tag{7}$$

$$\omega_{roll} = \frac{V_{syn} \cdot \sin\phi_{move} - H_y \cdot \dot{s}_h / (l_h + l_g)}{R_{link}} \tag{8}$$

In this study, we define the line passing through the mid-point of the grounding part as straight movement and the direction perpendicular to it as lateral movement, as shown in Fig.16a. Let ϕ_{st} and ϕ_{lat} be the angles between the x-axis and the direction of the straight and lateral movements, respectively. Parameters ϕ_{st} and ϕ_{lat} were obtained from the target shape of the robot, shown in Fig.16b, using H_x, H_y, and the length of the grounding part l_g, as follows:

$$\phi_{lat} = \tan^{-1}\frac{H_x + l_g}{H_y}, \tag{9}$$

$$\phi_{st} = \phi_{lat} + \frac{\pi}{2}. \tag{10}$$

By substituting ϕ_{st} and ϕ_{lat} to ϕ_{move} in (7) and (8), the shift velocity $\dot{s}_h$ and the angular velocity of rolling ω_{roll} for straight and lateral movements were be obtained.

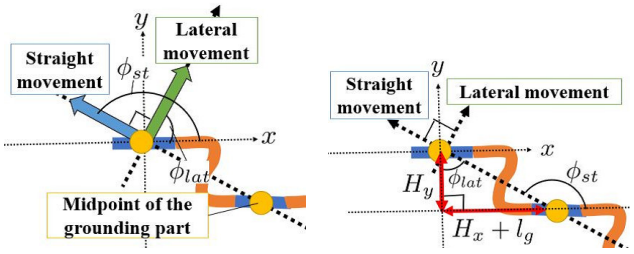

(a) Direction of straight and lateral movement

(b) Derivation of ϕ_{st} and ϕ_{lat}

Fig. 16. Straight and lateral movement.

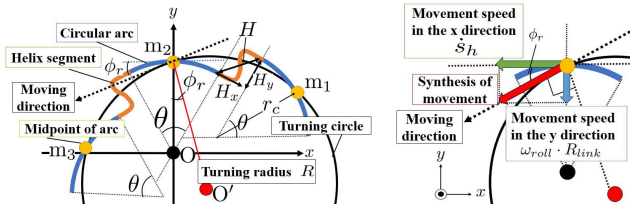

(a) (b)

Fig. 17. Relationship between shift and rolling when turning. (a) Definition of turning circle and the direction of movement when turning. The circle connecting the midpoint of circular arcs is the turning circle and the tangent direction of this circle is the direction of movement. (b) Synthesis of movement by shift control and rolling motion. The tangential direction of the turning circle is the direction of synthesis of movement using shift control and rolling motion.

Next, the turning movement is explained as follows. As shown in Fig.3b, the turning movement was realized by changing the target shape of the grounding part to circular arc shapes and performing shift control and rolling motion simultaneously. As shown in Fig.17a, the turning circle is determined by connecting the midpoint of three or more circular arcs, and the direction of movement during turning is the tangential direction of the turning circle. In this case, the circle passing through the midpoints of the three circular arc segments m_1–m_3, with a radius R, is considered the turning circle. The relationship between the velocity of the shift control and the rolling motion for turning can be determined by ϕ_r, which is the angle between the tangent lines of the circular arc and the turning circle. ϕ_r can be obtained using the vectors $\overrightarrow{\mathrm{m_2O}}$ and $\overrightarrow{\mathrm{m_2O'}}$ as follows:

$$\phi_r = \cos^{-1} \frac{\overrightarrow{\mathrm{m_2O}} \cdot \overrightarrow{\mathrm{m_2O'}}}{|\overrightarrow{\mathrm{m_2O}}||\overrightarrow{\mathrm{m_2O'}}|}. \tag{11}$$

where O and O′ are the centers of the circular arc and turning circle, respectively. As shown in Fig.17b, the velocity relationship in the x and y axes is obtained as follows:

$$\dot{s}_h \cdot \tan\phi_r = \omega_{roll} \cdot R_{link}. \tag{12}$$

By arbitrarily setting one of $\dot{s}_h$ or ω_{roll}, the other value of the turning movement can be obtained from (12).

III. EXPERIMENT

To confirm the effectiveness of the proposed method, we conducted experiments using the snake robot developed by Takemori [5], which is shown in Fig.18. The robot has 40 joints; each link length is 70 mm, the radius of the link is 28 mm, and the mass of the link is 146 g. The coefficient of static friction against the pipe and against the ground are 0.109 and 0.225, respectively, for the robot. The changes in the body shape and the switching of each motion were performed by an operator using a keyboard. In the experiment, the velocity of movement in a flat environment without obstacles was set as $V_{syn} = 0.005$ m/s and the shift velocity during the obstacle-aided locomotion was set as $\dot{s}_h = 0.015$m/s.

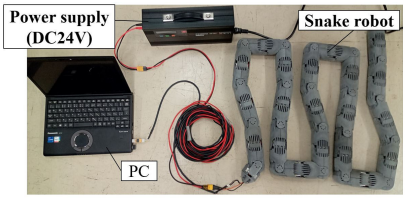

Fig. 18. Snake robot.

A. Obstacle-Aided Locomotion

Several obstacles with a diameter of 0.22 m were placed on the ground, and the robot performed obstacle-aided locomotion while adapting to the environment by extending, shortening, and bending the grounding part as well as reversing and adjusting the height of the obstacle-contacting part. After passing through the obstacles, the robot performed straight movement, lateral movement, and turning movement in a flat environment. The results are presented in Fig.19. In this experiment, the obstacles are numbered from 1 to 5 in order starting from the right. The ground on which they are placed is defined as the $x-y$ plane, and the center of Obstacle 1 is the origin. The (x, y) coordinates (mm) of Obstacles 1 to 4 were (0, 0), (520, 420), (650, 740), and (700, 1250), respectively. Obstacle 5 bridges between (1200, 1380) and (1200, 450), and the height from the ground to the center of the obstacle is 250 mm. The obstacles were placed at various intervals such that the robot could perform obstacle-aided locomotion while remaining in contact with two or more obstacles. Note that the body shapes were to be changed only when the first segment of the robot was the obstacle-contacting part.

First, in the elapsed time $t = 0$–10 s during the experiment, the obstacle-contacting part was reversed to get in contact with the obstacle located on the opposite side of the basic shape. At $t = 10$–15 s, the grounding part was shortened until the first obstacle-contacting part was in contact with Obstacle 3. After that, obstacle-aided locomotion was performed using shift control. At $t = 25$ s, it was predicted that the leading helix would interfere with Obstacle 4 and could not be used for locomotion; therefore, the grounding part was extended as shown for $t = 25$–35 s. Because the distance between Obstacle 4 and the first grounding part had opened up, the grounding part was bent until it came into contact with Obstacle 4, as shown in $t = 35$–45 s. Then, to utilize the ungrounded Obstacle 5, the height of the obstacle-contacting part was increased until it contacted the obstacle at $t = 60$–75 s. After exiting the obstacle environment using Obstacles 5, the

robot moved in a flat environment using lateral, straight, and turning movements. For the transition from straight to turning movement, all the grounding parts were gradually bent while moving straight so that the transition to the turning motion could be made smoothly.

The experimental results confirmed that the robot could move forward with the obstacle-contacting part pushing against the obstacles on two-dimensional planes and ungrounded obstacles. Therefore, we demonstrated that the proposed shape was effective for realizing movement in a three-dimensional obstacle environment.

However, at $t = 95$s, when there was no obstacle on the travel direction and the robot was propelled only by contact with an obstacle on the rear side, the robot rotated and deviated from the target path. This is because the robot has more grounding parts forward of obstacle 5, which increases both the weight needed to be pushed out and the frictional force with ground. This causes the front grounding parts to stall in its propulsion and the propulsive force created by the rear side to be converted to a rotational force. Hence, the robot must always be in contact with multiple obstacles to inhibit rotation or allow the operator to control the traveling direction. However, when moving through the obstacle environment to a flat environment with no obstacles, as in this experiment, the robot moved in several directions by switching to a movement that combined shift control and rolling.

B. Moving in Flat Environment without Obstacles

Additionally, experiments of the robot moving in a flat environment without obstacles were also performed. In the experiments, a tape was attached to the floor along an approximate target path. For straight movement, as shown in Fig.20a, the robot followed the target path in the beginning but gradually deviated from the target path. One of the reasons is the discretization error in fitting the robot shape to the target curve. Another reason is that the body shape of the robot gradually collapsed because of friction with the ground or the effect of gravity. The experimental results of the lateral movement of the robot are shown in Fig.20b. We confirmed that the head of the robot moved laterally according to the target path. Fig.20c shows that the robot was able to turn in a circle for turning movement.

These results demonstrate that the proposed method can effectively realize the movement of a robot in a flat environment without obstacles.

IV. CONCLUSION

In this study, we developed a method for obstacle-aided locomotion using piecewise helixes, adaptation to obstacle environments by changing the body shape, and movement in a flat environment without obstacles by combining shift control and rolling. The experimental results show that the robot can move forward by pushing the obstacles and can adapt to the environment by changing its body shape. Furthermore, we confirmed that the proposed method can utilize not only obstacles on a two-dimensional plane but also ungrounded

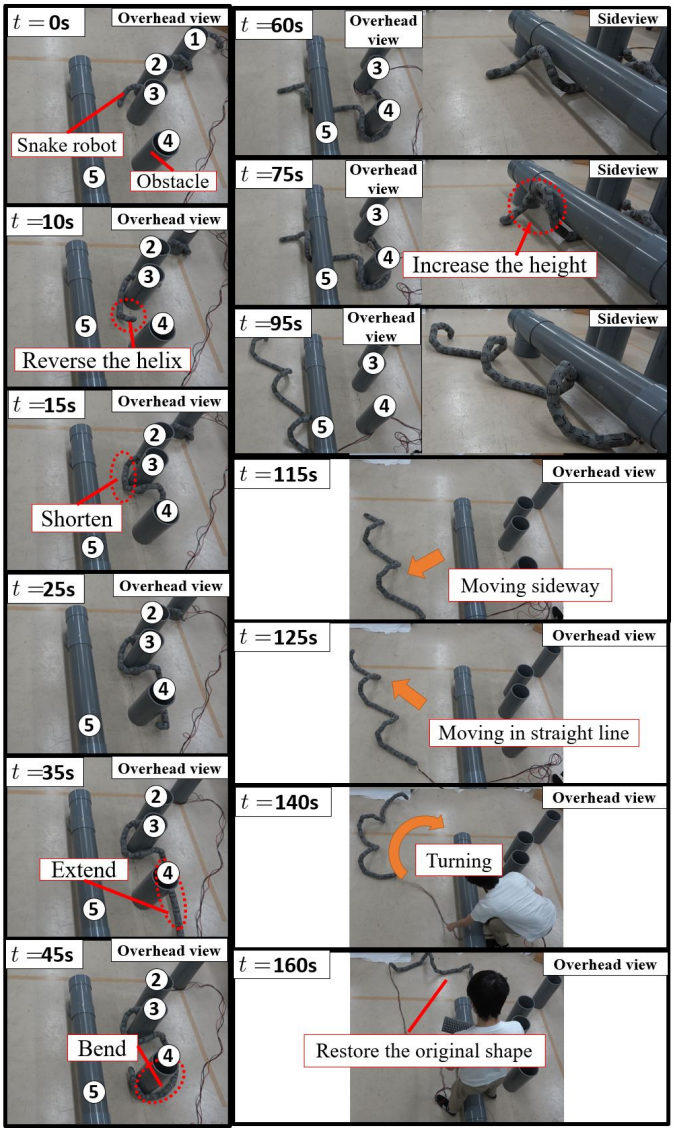

Fig. 19. Obstacle-aided locomotion and moving in an unobstructed environment.

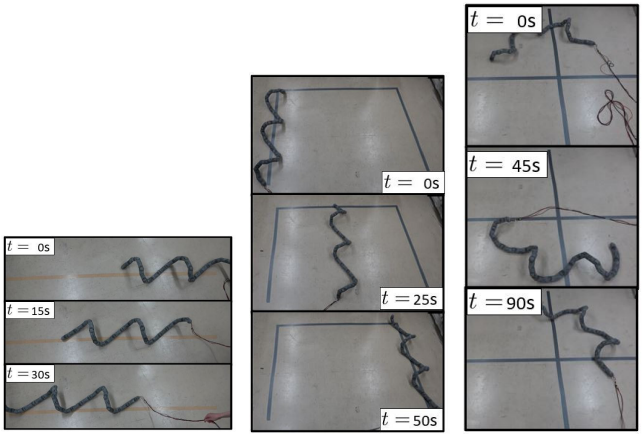

(a) Straight movement (b) Lateral movement (c) Turning movement

Fig. 20. Moving in unobstructed environment.

obstacles located at a height. For movement in a flat environment without obstacles, the direction of movement could be specified freely, and it was confirmed that the robot moved approximately in the specified direction.

The proposed method includes the obstacles located at high places into obstacle-aided locomotion, which had not been considered in previous studies. This will increase the number of obstacle options for non-wheeled snake robots to utilize for propulsion and contribute to further expansion of its exploration range. In addition, we proposed a method that can easily switch between obstacle-aided locomotion and movement in a flat environment without obstacles. This method can contribute to the expansion of the exploration range such that the snake robot can travel in different terrains. We used the control method of approximating the body shape of a snake robot to a continuous curve consisting of some simple shapes. This approach has not been used in previous studies for obstacle-aided locomotion. It enables the easy and intuitive operation of localized body shape changes, and adaptation to different obstacles and path selection. Moreover, this study is advantageous in that the target shape was divided into a grounding part and an obstacle-contacting part. The roles of each part were separated. Thus, the grounding part maintained the contact area with ground even when the height of the obstacle-contacting part was changed to ensure contact with an obstacle at a high place. This enabled the robot to perform movements in a stable posture without collapsing. Additionally, by using this contact area with the ground, it was proven that robots can move in a flat environment by combining of shift control and rolling.

In the future, we will introduce an automation control for the adaptation of robots to the environment. We will also improve the obstacle-contacting part of the robot by analyzing the dynamics of obstacle-aided locomotion and adapting the robot to more complex, three-dimensional environments, such as gaps and uneven ground.

REFERENCES

[1] S. Hirose and M. Mori, "Biologically Inspired Snake-like Robots," *Proc. IEEE Int. Conf. Intelligent Robots and Systems*, pp. 1-7, 2004.

[2] R. Ariizumi and F. Matsuno, "Dynamical Analysis of Sidewinding Locomotion by a Snake-Like Robot," *Proc. IEEE Int. Conf. Robotics and Automation*, pp. 5149-5154, 2013.

[3] K. Melo, "Modular Snake Robot Velocity for Side-Winding Gaits," *Proc. IEEE Int. Conf. Robotics and Automation*, pp.3716-3722, 2015.

[4] D. Rollinson and H. Choset, "Pipe Network Locomotion with a Snake Robot," *J. Field Robot.*, vol. 33, no. 3, pp. 322-336, 2016.

[5] T. Takemori, M. Tanaka, and F. Matsuno, "Ladder Climbing with a Snake Robot," *Proc. IEEE Int. Conf. Intelligent Robots and Systems*, pp. 8140-8145, 2018.

[6] M. Tanaka and K. Tanaka, "Control of a Snake Robot for Ascending and Descending Steps," *IEEE Trans. Robotics*, vol. 31, no. 2, 2015.

[7] A. A. Transeth, R. I. Leine, C. Glocker, K. Y. Pettersen, and P. Liljebäck, "Snake Robot Obstacle-Aided Locomotion: Modeling, Simulations, and Experiments," *IEEE Trans. Robotics*, vol. 24, no. 1, pp. 88-104, 2008.

[8] P. Liljebäck, K. Y. Pettersen, Ø. Stavdahl, and J. T. Gravdahl , "Hybrid Modelling and Control of Obstacle-Aided Snake Robot Locomotion," *IEEE Trans. Robotics*, vol. 26, no. 5, pp. 781-799, 2010.

[9] P. Liljebäck, K. Y. Pettersen, Ø. Stavdahl, and J. T. Gravdahl, "Experimental Investigation of Obstacle-Aided Locomotion with a Snake Robot," *IEEE Trans. Robotics*, vol. 27, no. 4, pp. 792-800, 2011.

[10] T. Kamegawa, R. Kuroki, M. Travers, and H. Choset, "Proposal of EARLI for the Snake Robot's Obstacle Aided Locomotion," *Proc. IEEE Int. Symp. Safety, Security, and Rescue Robotics*, 2012.

[11] T. Kamegawa, R. Kuroki, and A. Gofuku, "Evaluation of Snake Robot's Behavior Using Randomized EARLI in Crowded Obstacles," *IEEE Int. Symp. on Safety, Security, and Rescue Robotics*, 2014.

[12] M. Travers, J. Whitman, P. Schiebel, D. Goldman, and H. Choset, "Shape-based compliance in locomotion," *Proc. Robotics: Science and Systems*, 2016.

[13] T. Wang, J. Whitman, M. Travers, and H. Choset, "Directional Compliance in Obstacle-Aided Navigation for Snake Robots," *American Control Conference*, 2020.

[14] F. Ruscelli, G. Sartoretti, J. Nan, Z. Feng, M. Travers, and H. Choset, "Proprioceptive-Inertial Autonomous Locomotion for Articulated Robots," *Proc. IEEE Int. Conf. Robotics and Automation (ICRA)* , pp. 3436-3441, 2018.

[15] T. Sato, T. Kano, R. Kobayashi, and A. Ishiguro, "Snake-like Robot Driven by Decentralized Control Scheme for Scaffold-Based Locomotion," *Proc. IEEE/RSJ Int. Conf. Intelligent Robots and Systems*, pp. 132-138, 2012.

[16] H. Date and Y. Takita, "Adaptive Locomotion of a Snake Like Robot Based on Curvature Derivatives," *Proc. IEEE/RSJ Int. Conf. Intelligent Robots and Systems*, pp. 3554-3559, 2007.

[17] T. Kano and A. Ishiguro, "Obstacles Are Beneficial to Me! Scaffold-based Locomotion of a Snake-like Robot using Decentralized Control," *Proc. IEEE/RSJ Int. Conf. Intelligent Robots and Systems*, pp. 3273-3278, 2013.

[18] T. Kano, R. Kobayashi, and A. Ishiguro, "Tegotae-based Decentralised Control Scheme for Autonomous Gait Transition of Snake-like Robots," *Bioinspiration and Biomimetics* , vol. 12, 2017.

[19] W. Zhen, C. Gong and H. Choset, "Modeling Rolling Gaits of A Snake Robot," *Proc. IEEE Int. Conf. Robotics and Automation*, pp.3741-3746, 2015.

[20] M. Vespignani, K. Melo, S. Bonardi, and A. J. Ijspeert, "Role of Compliance on the Locomotion of a Reconfigurable Modular Snake Robot," *Proc. IEEE Int. Conf. intelligent Robots and Systems*, pp.2238-2245, 2015.

[21] Q. Fu , H. C. Astley and C. Li, "Snakes combine vertical and lateral bending to traverse uneven terrain," *Bioinspiration & Biomimetics* , vol. 17, no. 3, 2022.

[22] H. C. Astley, J. M. Rieser, A. Kaba, V. M. Paez, I. Tomkinson, J. R. Mendelson III, and D. I. Goldman, "Side-impact collision: mechanics of obstacle negotiation in sidewinding snakes," *Bioinspiration & Biomimetics* , vol. 15, no. 6, 2020.

[23] C. Gans, "Terrestrial locomotion without limbs," *Am. Zool.*, vol. 2, no.2, pp. 167-182, 1962.

[24] T. Takemori, M. Tanaka, and F. Matsuno, "Gait Design for a Snake Robot by Connecting Curve Segments and Experimental Demonstration," *IEEE Trans. Robotics*, vol. 34, no. 5, pp. 1384-1391, 2018.

[25] H. Yamada and S. Hirose, "Study of Active Cord Mechanism Approximations to Continuous Curves of a Multi -joint Body," (in Japanese), *Journal of the Robotics Society of Japan*, vol. 26, no. 1, pp. 110-120, 2008.